

## Neutron Capture on $^{180}\text{Ta}^m$ : Clue for an $s$ -Process Origin of Nature's Rarest Isotope

K. Wisshak,<sup>1,\*</sup> F. Voss,<sup>1</sup> C. Arlandini,<sup>1</sup> F. Bečvář,<sup>2</sup> O. Straniero,<sup>3</sup> R. Gallino,<sup>4</sup> M. Heil,<sup>1</sup> F. Käppeler,<sup>1</sup> M. Krtička,<sup>2</sup> S. Masera,<sup>4</sup> R. Reifarth,<sup>1</sup> and C. Travaglio<sup>5</sup>

<sup>1</sup>Forschungszentrum Karlsruhe, Institut für Kernphysik, Postfach 3640, D-76021 Karlsruhe, Germany

<sup>2</sup>Faculty of Mathematics and Physics, Charles University, CZ-180 00 Prague, Czech Republic

<sup>3</sup>Osservatorio Astronomico di Collurania, I-64100 Teramo, Italy

<sup>4</sup>Dipartimento di Fisica Generale, Università di Torino and INFN, Sezione di Torino, Via P. Giuria 1, I-10125 Torino, Italy

<sup>5</sup>Max-Planck Institut für Astronomie, Königstuhl 17, D-69117 Heidelberg, Germany

(Received 19 July 2001; published 30 November 2001)

The neutron capture cross section of  $^{180}\text{Ta}^m$  has been measured in the keV range, yielding a stellar average of  $1465 \pm 100$  mb at  $kT = 30$  keV. Though the sample contained only 6.7 mg  $^{180}\text{Ta}^m$  (at an enrichment of 5.5%), the few capture events could be separated from much larger backgrounds by a unique combination of high efficiency, good energy resolution, and high granularity of the Karlsruhe  $4\pi$  BaF<sub>2</sub> detector. A detailed  $s$ -process analysis based on this first experimental value indicates that  $^{180}\text{Ta}^m$  is predominantly of  $s$ -process origin.

DOI: 10.1103/PhysRevLett.87.251102

PACS numbers: 25.40.Lw, 26.20.+f, 27.70.+q, 97.10.Cv

For two reasons  $^{180}\text{Ta}^m$  is a unique nucleus: It is the rarest stable isotope found in the solar system, and it is the only isotope that is stable in the isomeric state. The rarity of  $^{180}\text{Ta}^m$  reflects the difficulty of its production. In fact, at first glance the common processes for synthesizing the heavy elements, including the  $s$ ,  $r$ , and  $p$  processes, seem to fail in this case. Apart from the difficulty of producing it,  $^{180}\text{Ta}^m$  may be even easily destroyed in the hot stellar interior by thermally induced depopulation to the short-lived ground state.

Obviously,  $^{180}\text{Ta}^m$  owes its existence to a subtle balance of nuclear and stellar parameters. Therefore, the actual abundance provides a sensitive test for nucleosynthesis models of the heavy elements. This feature has attracted continuous interest for nuclear physics as well as for astrophysics reasons. Apart from a possible  $s$ -process origin [1], the production of  $^{180}\text{Ta}^m$  in supernovae was proposed for the  $p$  process [2] as well as for the  $\nu$  process [3]. For a determination of the relative contributions from the various sites, the  $s$  process appears most suited for a quantitative discussion. As far as the astrophysical part is concerned the  $s$ -process scenarios are comparably stable and easier to model than supernovae.

Neutron capture nucleosynthesis in the  $s$  process is characterized by typical reaction times of  $\approx 1$  yr, slow compared to average  $\beta$  decays. This implies that the reaction chain follows the valley of stability and that the resulting abundances are to good approximation inversely proportional to the respective  $(n, \gamma)$  cross sections. Figure 1 shows that the main  $s$ -process reaction path (thick arrows) is bypassing  $^{180}\text{Ta}^m$  via the  $(n, \gamma)$  sequence along the stable hafnium isotopes, with only marginal feeding by two minor branchings. The decay of the  $8^-$  isomer in  $^{180}\text{Hf}$ , which is weakly populated by neutron capture on  $^{179}\text{Hf}$ , has been shown to account for about 20% of the observed  $^{180}\text{Ta}^m$  abundance [4,5]. This contribution is well determined by the partial cross section to  $^{180}\text{Hf}^m$ .

The second branching to  $^{180}\text{Ta}^m$  occurs via neutron captures on  $^{179}\text{Ta}$  which in turn is produced by  $\beta$  decay of the  $7/2^-$  state at 214 keV in  $^{179}\text{Hf}$  [6]. Since this state can be thermally populated in the stellar photon bath only at sufficiently high temperatures, this route may, therefore, be interpreted as a sensitive stellar thermometer [1].

This second branching being open only at relatively high temperatures raises the possibility that the produced  $^{180}\text{Ta}^m$  may not survive because it could be immediately destroyed by thermally induced transitions to the short-lived ground state [1]. Though direct decay by internal transitions is prohibited by selection rules, excitation of a mediating, excited state with decay channels to the ground state may suffice for efficient depopulation. Many attempts to locate the position of the lowest mediating state, which determines the temperature dependence of the  $^{180}\text{Ta}^m$  half-life, were hampered by limited experimental sensitivities.

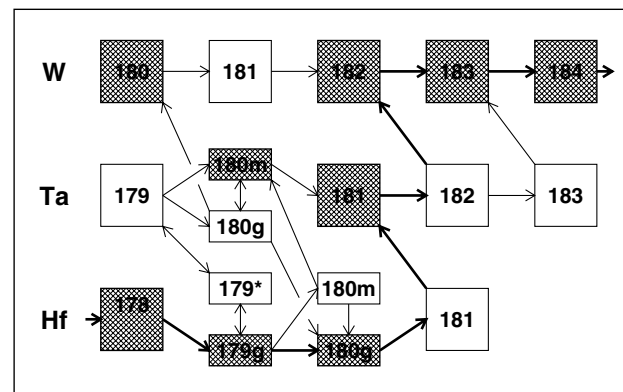


FIG. 1. The reaction path of the  $s$  process in the Hf/Ta/W region. Though the main reaction path (thick arrows) is bypassing  $^{180}\text{Ta}^m$ , this rare isotope can, in fact, be produced by neutron captures on  $^{179}\text{Ta}$  and  $\beta$  decays of a weakly populated isomer in  $^{180}\text{Hf}$ , which are the result of minor branchings at  $A = 179$  and 180.

This problem could recently be solved by a photoactivation measurement [7] using the world supply of enriched tantalum, a sample consisting of 150 mg oxide powder with a  $^{180}\text{Ta}^m$  content of only 5.5%. With this sample and some other improvements the sensitivity of previous experiments based on natural samples ( $^{180}\text{Ta}^m/^{181}\text{Ta} = 1.2 \times 10^{-4}$ ) could be increased by a factor of 5000.

The lowest of several newly identified mediating states at 1.01 MeV excitation energy can, indeed, be reached at typical  $s$ -process temperatures with the consequence that  $^{180}\text{Ta}^m$  cannot survive in the constant temperature scenario of the classical  $s$  process [7]. Instead, it was found that the highly convective situation during He shell flashes in the Red Giant phase of stellar evolution favors the  $s$ -process production of  $^{180}\text{Ta}^m$ . In these so-called asymptotic giant branch (AGB) stars, recurrent thermal pulses give rise to rapid mixing of freshly synthesized material into cooler zones.

In this Letter we report the first measurement of the stellar  $(n, \gamma)$  cross section of  $^{180}\text{Ta}^m$ , the most crucial information for determining the  $s$ -process yield. Up to now, the available results from statistical model calculations differed by a factor of 2 [1,8–11], reflecting the 50% uncertainty typical of this technique.

The measurement was carried out in the neutron energy range from 10 to 100 keV using gold as a standard. Neutrons were produced via the  $^7\text{Li}(p, n)^7\text{Be}$  reaction with the pulsed proton beam of 0.7 ns width, 250 kHz repetition rate, and 2  $\mu\text{A}$  average current from the Karlsruhe 3.7 MV Van de Graaff accelerator. The neutron energy was determined by time of flight (TOF), the samples being located at a flight path of 79 cm. The proton energy was adjusted 30 keV above the reaction threshold resulting in a continuous neutron spectrum from 10 to 100 keV. Capture events were detected with the Karlsruhe  $4\pi$  BaF<sub>2</sub> array [12] by registration of the prompt capture  $\gamma$ -ray cascades. The detector array consists of 41 hexagonal and pentagonal crystals forming a spherical shell of BaF<sub>2</sub> with 10 cm inner radius and 15 cm thickness. It is characterized by a resolution in  $\gamma$ -ray energy of 7% at 2.5 MeV, a time resolution of 500 ps, and an efficiency of 99% and 95% for the detection of capture events in  $^{180}\text{Ta}^m$  and gold, respectively.

The sample of the before mentioned photoactivation experiment has been used in this work as well. Because of its enormous value, the powder was safely enclosed in a graphite container of 22 mm diameter with  $\approx 1$  mm thick walls. The successful TOF measurements at keV energies on only 6.7 mg  $^{180}\text{Ta}^m$  in the presence of a dominant  $^{181}\text{Ta}$  matrix were particularly challenging and highlights the advantage of the  $4\pi$  BaF<sub>2</sub> array, i.e., the combination of good energy resolution, high  $\gamma$  efficiency, sufficient granularity, and low neutron sensitivity. Figure 2 illustrates that these features were essential for separating the few captures on  $^{180}\text{Ta}^m$  from the bulk of events from  $^{181}\text{Ta}$ , using the differences in neutron separation energies ( $B_n = 7.58$  MeV for

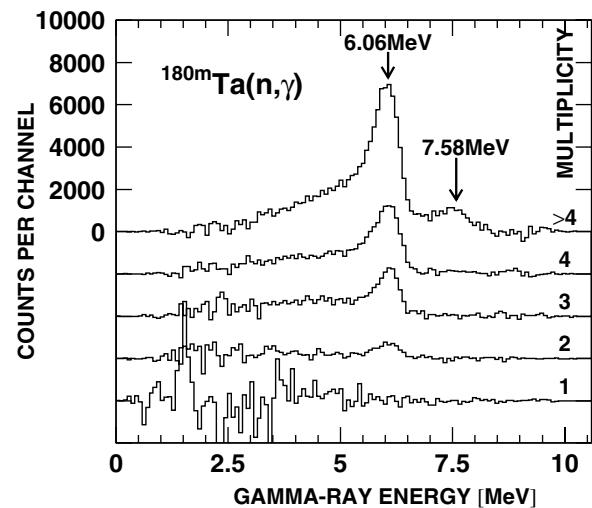


FIG. 2. Deposited  $\gamma$ -ray energy for prompt capture cascades of different multiplicities. The spectra are dominated by the 6.06 MeV line from capture on  $^{181}\text{Ta}$ , but  $^{180}\text{Ta}^m$  events are clearly concentrated in the spectrum with multiplicity  $>4$ .

$^{180}\text{Ta}^m$  compared to 6.06 MeV for  $^{181}\text{Ta}$ ) and in cascade multiplicities. Furthermore, the background problem due to neutrons scattered in the graphite container was strongly reduced by the excellent TOF structure of the experiment, which caused a significant delay of this component compared to the distribution of true events.

The enriched tantalum sample and a set of additional samples in identical graphite containers were mounted on a sample ladder: a gold disk for determining the neutron flux, a natural tantalum sample to account for the effect of  $^{181}\text{Ta}$ , as well as an empty container and an empty position for measuring various background components. The samples were changed in intervals of about 10 min. The total beam time of the experiment was 45 days.

Figure 2 shows the background subtracted  $\gamma$  spectra of capture events from the enriched Ta sample. Though dominated by the 6.06 MeV line due to capture events from  $^{181}\text{Ta}$ , neutron captures on  $^{180}\text{Ta}^m$  are clearly observed in the spectrum with multiplicity  $>4$ . The separation of both components was performed (i) by a fit based on a parameter systematics for spectra shapes from analyses of neutron capture measurements on more than 50 other isotopes and (ii) by deriving the  $^{181}\text{Ta}$  contribution from the data recorded with the natural sample. Both results were consistent within  $\pm 2.5\%$ . The separation obtained by the first procedure is illustrated in Fig. 3.

The fraction of  $^{180}\text{Ta}^m$  events represented in the spectrum with multiplicity  $>4$  was determined by a simulation of the experiment using the GEANT code [13]. The geometry of the  $4\pi$  BaF<sub>2</sub> array was modeled in full detail including the 41 crystals with reflectors and all structural materials [14]. The efficiency for  $\gamma$  rays originating from a sample in the center of the array was calculated including the corrections for  $\gamma$ -ray self-absorption and for conversion electrons. The proper energy resolution was

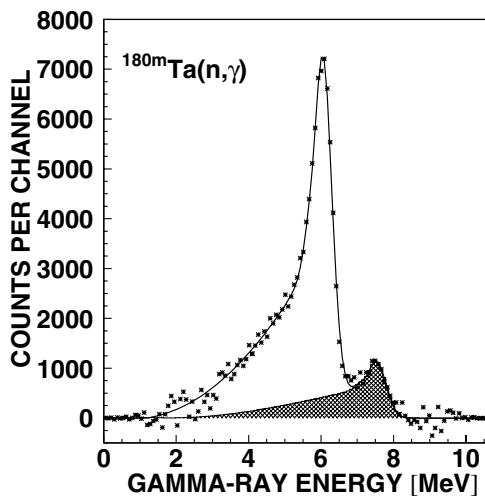


FIG. 3. Deposited  $\gamma$ -ray energy for prompt capture cascades from the investigated  $^{180}\text{Ta}^m$  sample for multiplicities  $>4$  and neutron energies between 50 and 100 keV. The  $^{180}\text{Ta}^m$  and  $^{181}\text{Ta}$  components are separated by the fit procedure described in the text.

adopted from experimental information recorded with an analog-to-digital converter system.

Gamma-ray cascades from  $(n, \gamma)$  reactions were calculated for  $^{180}\text{Ta}^m$ ,  $^{181}\text{Ta}$ , and  $^{197}\text{Au}$  with the Monte Carlo code CASINO [15], the implementation of the DICEBOX algorithm [16] for the keV neutron capture regime. An important feature of this code is the proper treatment of the probability for emission of conversion electrons. With these calculated  $\gamma$ -ray cascades the response of the  $4\pi$  BaF<sub>2</sub> detector was determined in the GEANT simulations by following the energy deposited in the individual modules down to the experimental threshold of  $\sim 50$  keV.

Within experimental uncertainties, the measured spectra for different multiplicities could be reproduced for  $^{181}\text{Ta}$  [17], and  $^{197}\text{Au}$ , thus providing a reliable extrapolation for  $^{180}\text{Ta}^m$ . Accordingly, the  $^{180}\text{Ta}^m$  spectrum with multiplicity  $>4$  was found to represent 83% of all capture events, in good agreement with the estimated  $87 \pm 5\%$  based on the experimental data of Fig. 2.

The final results for the stellar cross sections are summarized in Table I (for a full description of the experiment and detailed numerical values, see Ref. [17]). The systematic uncertainty of 5.1% reflects the difficulty in separating true  $^{180}\text{Ta}^m$  events from the  $^{181}\text{Ta}$  component. The comparison with theoretical predictions shows that the cross section is significantly smaller than the value of Ref. [1], which had been adopted previously.

As mentioned before, the result of the photoactivation measurement [7] implies that  $^{180}\text{Ta}^m$  cannot be accounted for by the classical  $s$  process [1], but that it can be produced in substantial amounts by the more complex scenarios related to the  $s$  process during recurrent thermal instabilities in the AGB phase of 1.5 to 3  $M_{\odot}$  mass stars [18–20]. In this model, about 95% of the neutron irradiation occurs via the  $^{13}\text{C}(\alpha, n)$  reaction between thermal instabilities at

TABLE I. Stellar neutron capture cross section of  $^{180}\text{Ta}^m$  compared to previous calculations.

	$kT$ (keV)	$\langle\sigma v\rangle/v_T$ (mb)	Uncertainty (mb)		
			stat.	syst.	tot.
Expt.	10	2695	153	137	205
Expt.	30	1465	66	75	100
Calc.	30	2662 [1], 3270 [8], 2273 [9], 1800 [10], 1705 [11]			

comparably low temperatures of  $T_8 = 1$  (temperature in units of  $10^8$  K), where  $^{179}\text{Hf}$  and  $^{180}\text{Ta}^m$  are both stable and where only a minor fraction of  $^{180}\text{Ta}^m$  is produced via the decay of  $^{180}\text{Hf}^m$ . During thermal instabilities, however, temperatures of  $T_8 = 2.5$ – $2.8$  are reached for a few years, resulting in a second neutron burst due to the marginal activation of the  $^{22}\text{Ne}(\alpha, n)$  reaction. At these higher temperatures,  $^{179}\text{Hf}$  becomes unstable, thus opening the neutron capture sequence from  $^{179}\text{Ta}$  to  $^{180}\text{Ta}^m$ . The prolific energy production in the He shell flashes creates a highly convective zone with turnover times of less than a few hours. This means that mixing of freshly produced  $^{180}\text{Ta}^m$  from the bottom of the convective zone into cooler regions occurs so fast that  $^{180}\text{Ta}^m$  survives even if one adopts the lower limit of the half-lives deduced from the photoactivation experiment [7]. Soon after the He shell flash, the reaction zone is partly engulfed by the convective envelope where the  $^{180}\text{Ta}^m$  is temporarily stored before it is ejected into the interstellar medium at the end of the AGB phase.

According to the result of the photoactivation measurement [7] the large gradient in temperature ( $0.2 \leq T_8 \leq 3$ ) and density ( $10 \leq \rho \leq 10^4$  g cm<sup>-3</sup>) implies that the effective lifetime of  $^{180}\text{Ta}^m$  varies by more than 15 orders of magnitude between the top and the bottom of the convective zone. In the present stellar model calculations, the production and survival of  $^{180}\text{Ta}^m$  was followed in detail by dividing this convective zone into 25 meshes of equal extension, where the physical conditions could be considered constant during each time step. The evolution of each mesh with time was obtained by the stellar model, which accounts also for the changes from one He shell flash to the next along the AGB evolution [20]. The nucleosynthesis was followed in each mesh separately, and the resulting abundances were periodically mixed to account for the turnover time of the convective zone.

It is evident that high temperatures prevail only in a relatively thin layer near the bottom of the convective zone, where also the  $s$  process takes place. It is only there that  $^{180}\text{Ta}^m$  can be efficiently destroyed via thermally induced transitions to the short-lived ground state. However, as long as the turnover time is short compared to the actual half-life, most of the produced  $^{180}\text{Ta}^m$  is rapidly brought to the outer and cooler layers of the convective zone where it survives unaltered. In view of the very short turnover time this condition is satisfied for the entire range of half-lives suggested in Ref. [7].

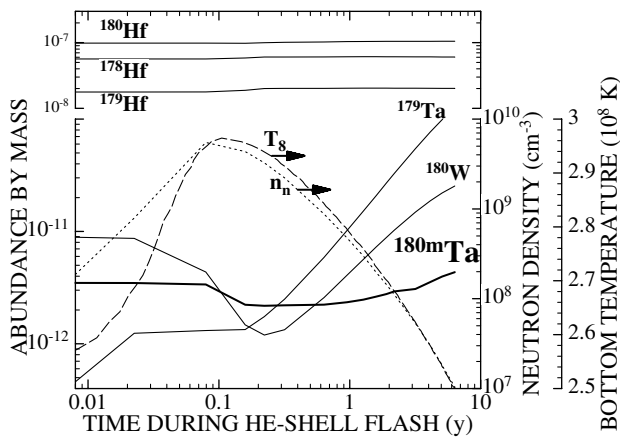


FIG. 4. Time evolution of abundances (as mass fractions) during the  $^{22}\text{Ne}(\alpha, n)^{25}\text{Mg}$  neutron burst for a typical advanced pulse of the standard model star ( $2M_{\odot}$ ,  $Z = 1/2 Z_{\odot}$ , solid lines). Compared to the evolution of the neighboring Hf isotopes, which are in reaction equilibrium, the variations of  $^{179}\text{Ta}$ ,  $^{180}\text{Ta}^m$ , and  $^{180}\text{W}$  are due to the branching at  $^{179}\text{Hf}$ . Since the  $^{180}\text{Ta}^m$  yields for stars of different mass and metallicity are very similar, the average over galactic chemical evolution is not expected to differ significantly from these results (see text). The dotted line corresponds to the bottom temperature of the convective region (right scale), which reflects also the behavior of the neutron density.

In contrast to the half-life problem, the experimental  $(n, \gamma)$  rate of  $^{180}\text{Ta}^m$  has a much deeper consequence since the  $s$ -process yields around  $A = 180$  are to good approximation inversely proportional to the respective Maxwellian-averaged cross sections. The experimental rate being nearly a factor of 2 smaller than the value adopted previously [1,7] implies a corresponding increase of the  $^{180}\text{Ta}^m$  production, reaching now  $\sim 85\%$  of the solar value.

The contribution to the  $^{180}\text{Ta}^m$  abundance resulting from the neutron burst by the  $^{22}\text{Ne}$  source averaged over a typical He shell flash is illustrated in Fig. 4. While the neighboring Hf isotopes are in reaction equilibrium and remain almost unchanged, the branching at  $^{179}\text{Hf}$  causes the  $^{179}\text{Ta}$  and  $^{180}\text{W}$  abundances to follow the temperature and neutron density profiles (with a certain delay due to the  $\beta^-$  decay half-life of the 214 keV level in  $^{179}\text{Hf}$ ). As a consequence of the complex interplay between temperature, neutron density, and  $\beta$  decay this behavior is less evident for the  $^{180}\text{Ta}^m$  abundance. Nevertheless, the initial  $^{180}\text{Ta}^m$  abundance in Fig. 4, which results from the neutron exposure by the  $^{13}\text{C}$  source in the interpulse phase and from previous He shell flash episodes, increases during the flash by 40%.

Starting from the situation illustrated in Fig. 4 the  $s$ -process production of  $^{180}\text{Ta}^m$  has been studied for a range of stellar masses ( $1.5 < M/M_{\odot} < 3$ ) and metallicities ( $0.01 < Z/Z_{\odot} < 1$ ). It turned out that the respective  $^{180}\text{Ta}^m$  yields are fairly independent of stellar mass and

metallicity, in particular, for stars around one-tenth of the solar metallicity, which are known to contribute most efficiently to the solar  $s$  abundances between Ba and Pb [21,22]. Since all investigated models predicted  $^{180}\text{Ta}^m$  abundances between 80% and 86% of the solar ratio, this range determines also the average over galactic chemical evolution. This result strongly suggests a predominant  $s$ -process origin of  $^{180}\text{Ta}^m$  related to the He shell burning phase of low mass AGB stars.

The main residual uncertainties in the  $s$ -process yield of  $^{180}\text{Ta}^m$  are due to the stellar half-life of  $^{179}\text{Hf}$  and the  $(n, \gamma)$  cross section of  $^{179}\text{Ta}$ . Variation of these quantities within plausible limits of  $\pm 30\%$  would change the  $^{180}\text{Ta}^m$  abundance by 15% and 25%, respectively. While the part of the half-life might be difficult to improve, a measurement of the  $^{179}\text{Ta}$  cross section remains an experimental challenge for a conclusive analysis of the  $s$ -process origin of  $^{180}\text{Ta}^m$ .

\*To whom correspondence should be addressed.

Email address: wisshak@ik3.fzk.de

- [1] Zs. Németh, F. Käppeler, and G. Reffo, *Astrophys. J.* **392**, 277 (1992).
- [2] M. Rayet *et al.*, *Astron. Astrophys.* **298**, 517 (1995).
- [3] S. E. Woosley *et al.*, *Astrophys. J.* **356**, 272 (1990).
- [4] H. Beer and R. A. Ward, *Nature (London)* **291**, 308 (1981).
- [5] S. E. Kellogg and E. B. Norman, *Phys. Rev. C* **46**, 1115 (1992).
- [6] K. Yokoi and K. Takahashi, *Nature (London)* **305**, 198 (1983).
- [7] D. Belic *et al.*, *Phys. Rev. Lett.* **83**, 5242 (1999).
- [8] J. A. Holmes *et al.*, *At. Data Nucl. Data Tables* **18**, 305 (1976).
- [9] M. J. Harris, *Astrophys. Space Sci.* **77**, 357 (1981).
- [10] H. Beer and R. L. Macklin, *Phys. Rev. C* **26**, 1404 (1982).
- [11] T. Rauscher and F.-K. Thielemann, *At. Data Nucl. Data Tables* **75**, 1 (2000).
- [12] K. Wisshak *et al.*, *Nucl. Instrum. Methods Phys. Res., Sect. A* **292**, 595 (1990).
- [13] J. Apostolakis, CERN, GEANT library (available from [www.cern.ch](http://www.cern.ch)).
- [14] M. Heil *et al.*, *Nucl. Instrum. Methods Phys. Res., Sect. A* **459**, 229 (2001).
- [15] F. Bečvář, in *Capture Gamma-Ray Spectroscopy and Related Topics*, edited by S. Wender, AIP Conf. Proc. No. 529 (AIP, Melville, NY, 2000), p. 504.
- [16] F. Bečvář, *Nucl. Instrum. Methods Phys. Res., Sect. A* **417**, 434 (1998).
- [17] K. Wisshak *et al.*, *Forschungszentrum Karlsruhe Report No. FZKA-6362*, 2000.
- [18] O. Straniero *et al.*, *Astrophys. J.* **440**, L85 (1995).
- [19] O. Straniero *et al.*, *Astrophys. J.* **478**, 332 (1997).
- [20] R. Gallino *et al.*, *Astrophys. J.* **497**, 388 (1998).
- [21] C. Travaglio *et al.*, *Astrophys. J.* **521**, 691 (1999).
- [22] C. Travaglio *et al.*, *Astrophys. J.* **549**, 346 (2001).